

Supporting information: Controls of intermodel uncertainty in land carbon sink projections

Ryan S. Padrón¹, Lukas Gudmundsson¹, Laibao Liu¹, Vincent Humphrey^{1,2}, Sonia I. Seneviratne¹

¹Institute for Atmospheric and Climate Science, Department of Environmental Systems Science, ETH Zurich, Zurich, 8092, Switzerland

²Department of Geography, University of Zurich, Zurich, Switzerland

Correspondence to: Ryan S. Padrón (ryan.padron@env.ethz.ch)

Model	SSP126	1pctCO2-bgc	Land surface model	Fire	Dynamic vegetation	Nitrogen cycle
ACCESS-ESM1-5	30	1	CABLE2.4 with CASA-CNP	No	No	Yes (and phosphorus)
CanESM5	50	1	CLASS-CTEM	No	No	No
CESM2	5	1	CLM5	Yes	No	Yes
CMCC-ESM2	1	1	CLM4.5	Yes	No	Yes
CNRM-ESM2-1	5	4	ISBA-CTRIP	Yes	No	Implicit
EC-Earth3-Veg	5	1	HTESSEL and LPJ-GUESS	Yes	Yes	Yes
GFDL-ESM4	1	1	LM4.1	Yes	Yes	No
IPSL-CM6A-LR	6	1	ORCHIDEE, branch 2.0	No	No	No
MPI-ESM1-2-LR	10	3	JSBACH3.2	Yes	Yes	Yes
NorESM2-LM	1	0	CLM5	Yes	No	Yes
UKESM1-0-LL	16	1	JULES-ES-1.0	No	Yes	Yes

Table S1: Information on the Earth system models employed in the analysis. The columns SSP126 and 1pctCO2-bgc indicate the number of realizations from each model per scenario. The main analysis focuses on the shared socio-economic pathway SSP126, whereas the 1pctCO2-bgc simulations are used to estimate the sensitivity of GPP to CO₂ concentration (sCO₂).

Model	Depth of the boundaries between soil moisture layers [m]
ACCESS-ESM1-5	0, 0.022, 0.08, 0.234, 0.643, 1.728, 4.6
CESM2	0, 0.025, 0.065, 0.125, 0.21, 0.33, 0.49, 0.69, 0.93, 1.21, 1.53, 1.89, 2.29, 2.745, 3.285, 3.925, 4.665, 5.505, 6.445, 7.485, 8.575
CMCC-ESM2	0, 0.0175, 0.0451, 0.0906, 0.1655, 0.2891, 0.4929, 0.8289, 1.3828, 2.2961, 3.8019, 6.2845, 10.3775, 17.1259, 28.2520, 42.1032
CNRM-ESM2-1	0, 0.01, 0.04, 0.1, 0.2, 0.4, 0.6, 0.8, 1, 1.5, 2, 3, 5, 8, 12
CanESM5	0, 0.1, 0.35, 4.1
EC-Earth3-Veg	0, 0.07, 0.28, 1, 2.89
GFDL-ESM4	0, 0.02, 0.06, 0.1, 0.15, 0.2, 0.3, 0.4, 0.6, 0.8, 1, 1.4, 1.8, 2.2, 2.6, 3, 4, 5, 6, 7.5, 10
IPSL-CM6A-LR	0, 0.001, 0.004, 0.01, 0.022, 0.045, 0.092, 0.186, 0.374, 0.75, 1.5, 2
MPI-ESM1-2-LR	0, 0.065, 0.319, 1.232, 4.134, 9.834
NorESM2-LM	0, 0.025, 0.065, 0.125, 0.21, 0.33, 0.49, 0.69, 0.93, 1.21, 1.53, 1.89, 2.29, 2.745, 3.285, 3.925, 4.665, 5.505, 6.445, 7.485, 8.575
UKESM1-0-LL	0, 0.1, 0.35, 1, 3

Table S2: Soil layer discretization of employed Earth system models.

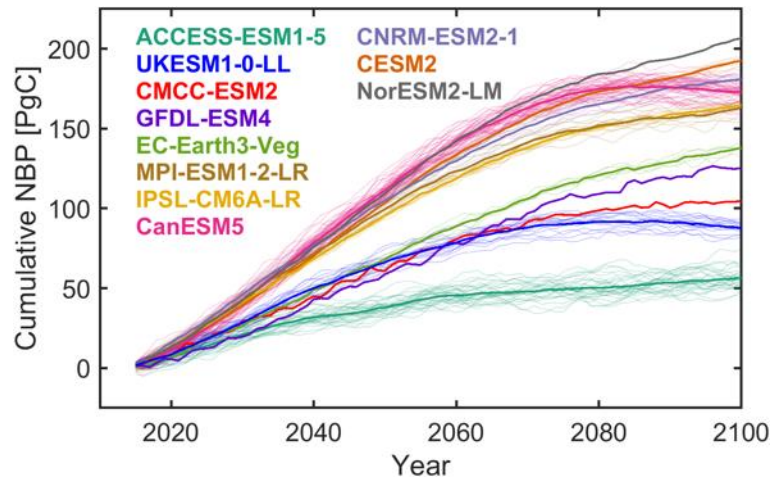


Figure S1: Projected global land NBP from different Earth system models and different realizations of individual models for scenario SSP126. The average value for each model is shown by the thicker lines, whereas thin lines represent single realizations. If a model does not have information over Greenland, NBP is set to zero. Cumulative global land NBP is estimated by multiplying the area-weighted average NBP times the land surface area excluding Antarctica ($135.22\text{E}6 \text{ km}^2$).

30

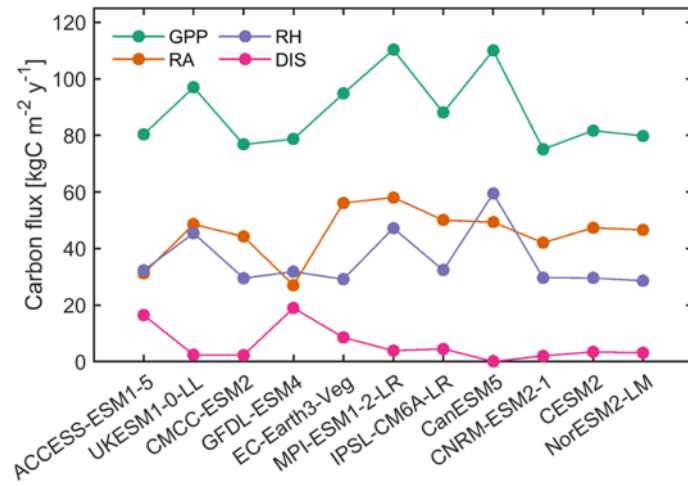
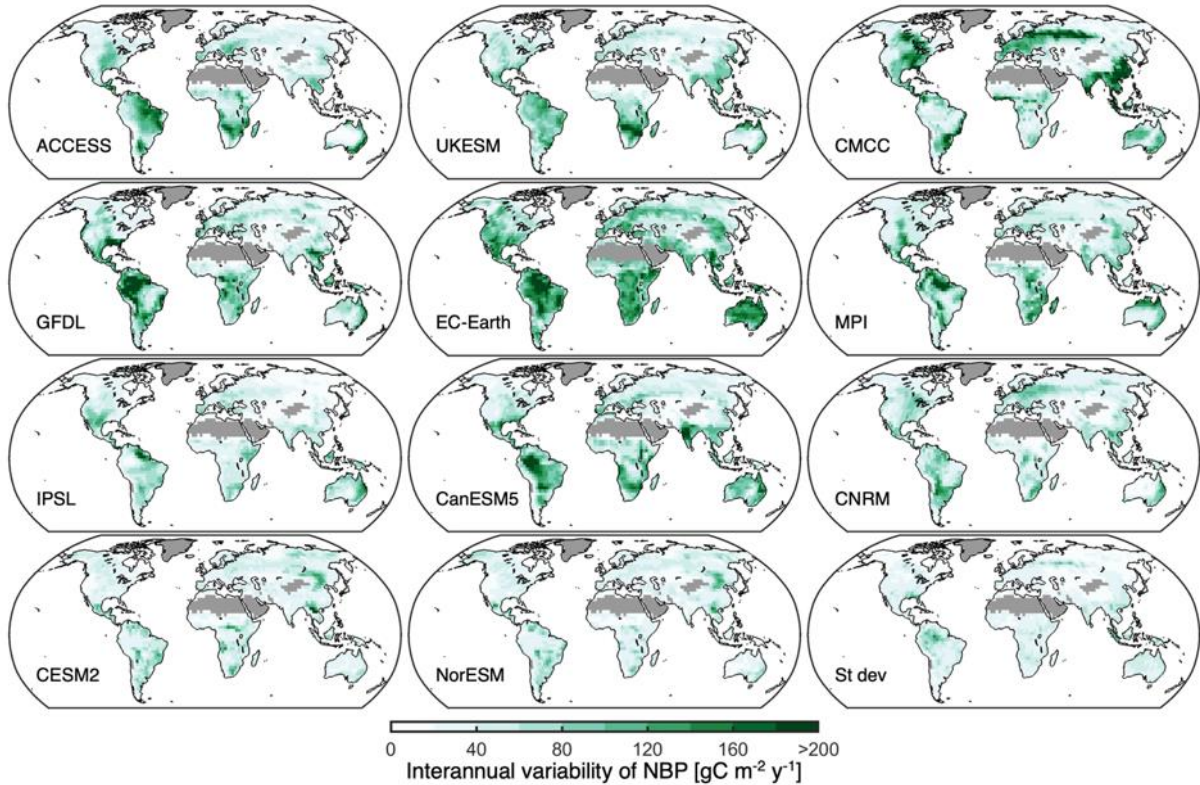
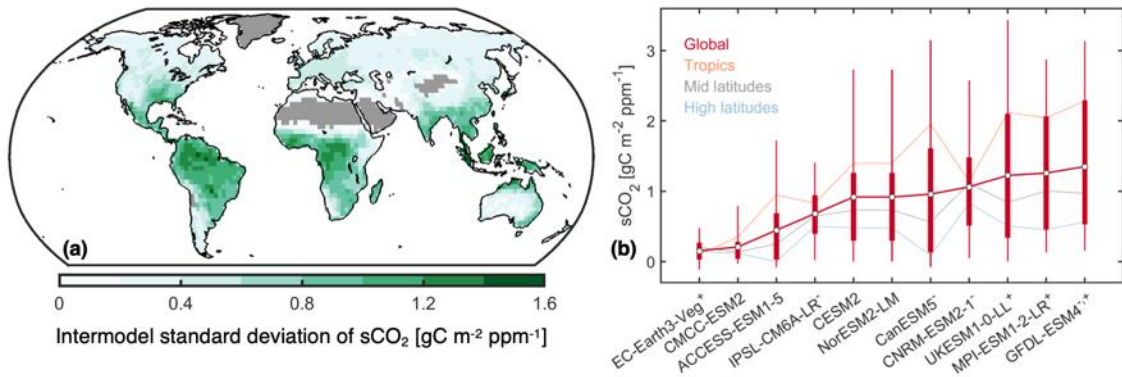


Figure S2: Projected gross primary production (GPP), autotrophic respiration (RA), heterotrophic respiration (RH), and ecosystem disturbances (DIS) such as fires per Earth system model. Long-term averages from the period 2015 to 2100 are shown. From left to right models are ordered according to increasing projected NBP. To increase model comparability, only grid cells where all models have information are considered. If a model does not have information over Greenland, NBP is set to zero.

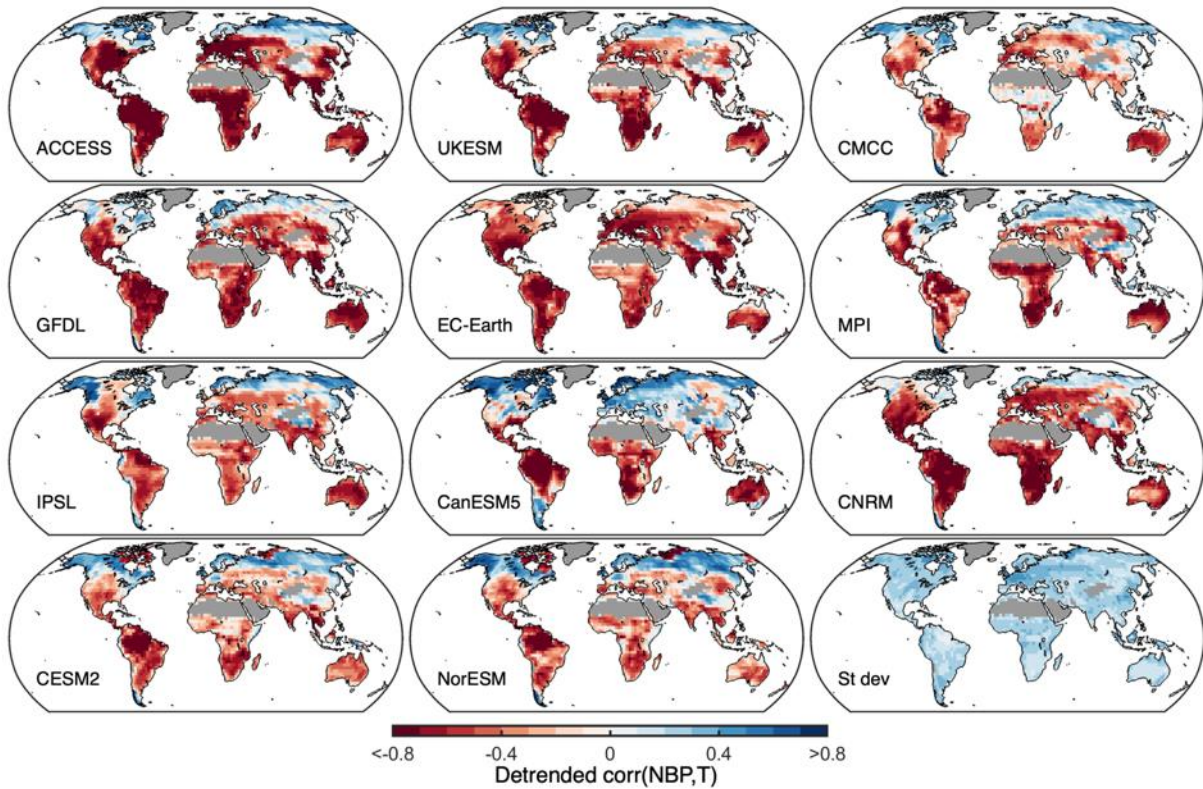


35

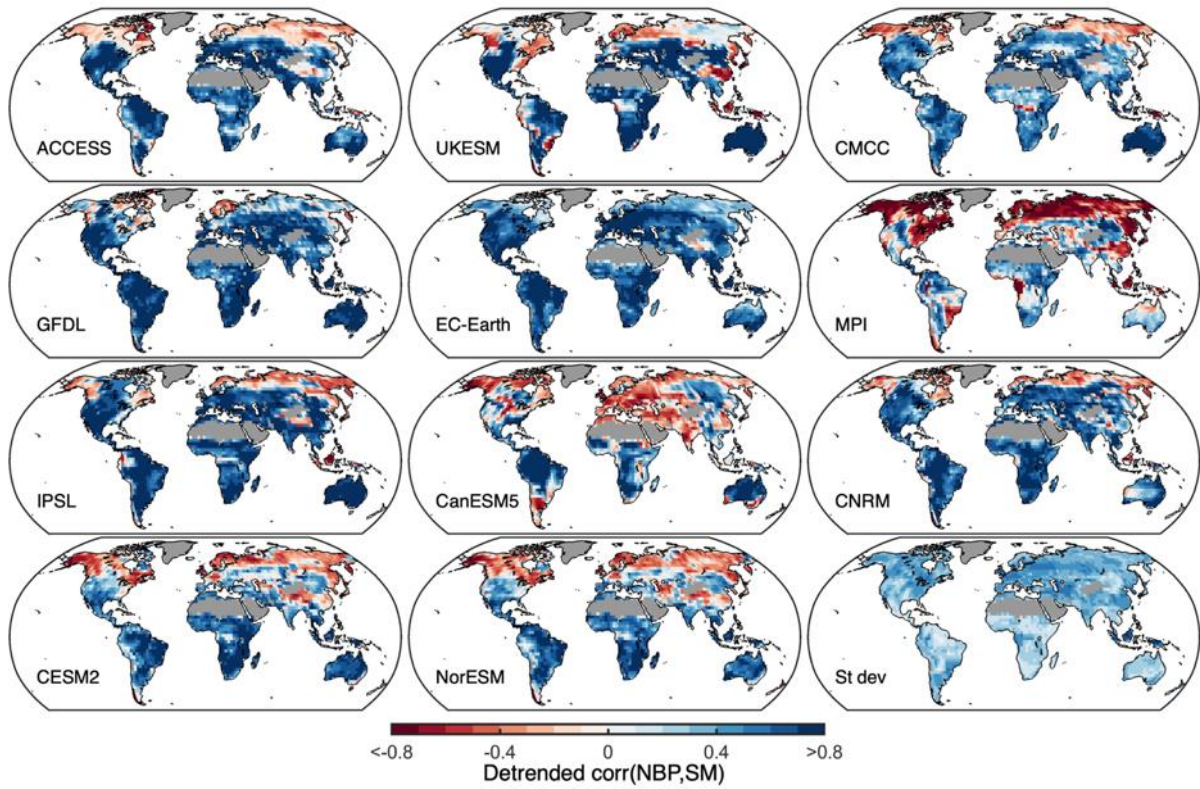
Figure S3: Intermodel differences in interannual NBP variability. Maps of the standard deviation from annual detrended projected NBP during 2015 to 2100 from individual models. The intermodel standard deviation is shown at the bottom right. Greenland and desert regions are masked.



40 **Figure S4: Intermodel differences in the sensitivity of GPP to atmospheric CO_2 concentration ($s\text{CO}_2$).** (a) Intermodel standard deviation of $s\text{CO}_2$. (b) Distribution of $s\text{CO}_2$ from all land grid cells. Antarctica, Greenland, and desert regions are omitted. The marker indicates the median $s\text{CO}_2$, the boxes span the interquartile range, and the whiskers span from the 5th to the 95th percentile. Additional lines indicate the median $s\text{CO}_2$ from land grid cells across the tropics, mid latitudes, and high latitudes. Models that do not include a nitrogen cycle are indicated by (*) and models that include dynamic vegetation are indicated by (+).

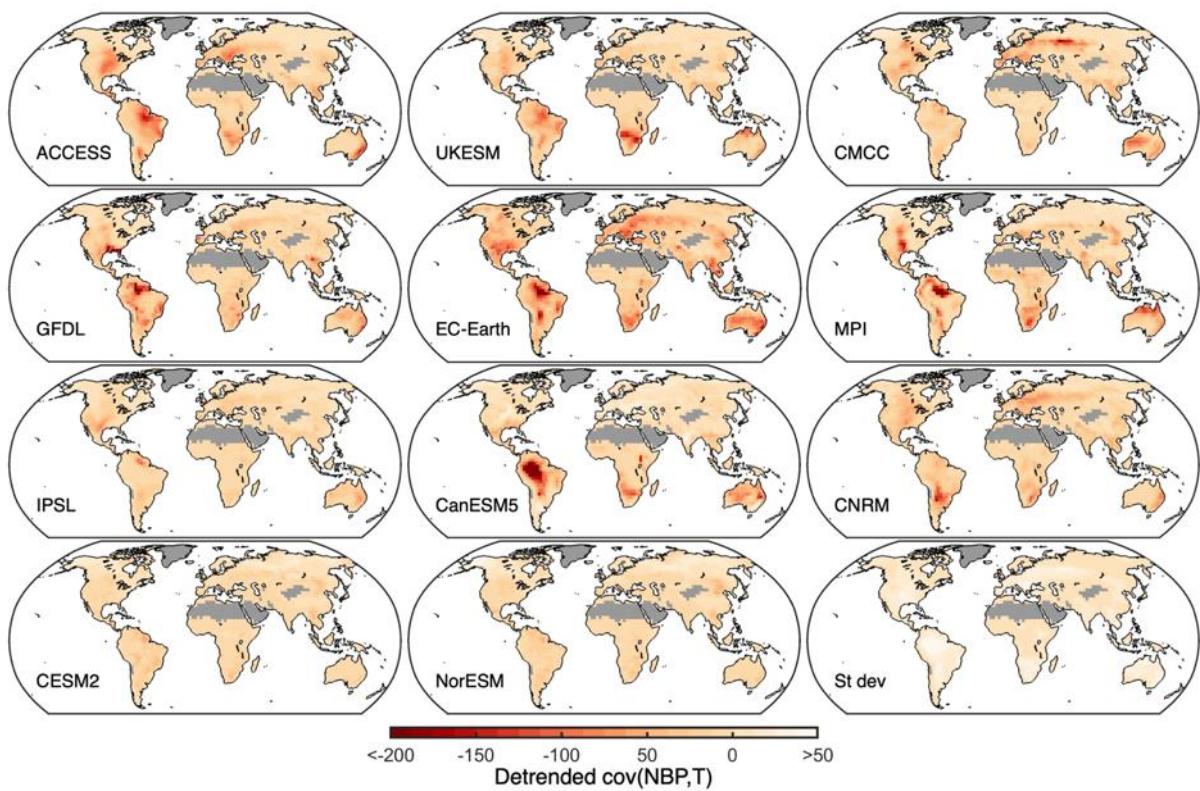


45 **Figure S5: Intermodel differences in the interannual correlation between detrended NBP and temperature.** The correlation is computed from the detrended time series of annual average NBP and annual average warm season T. In the extratropics (latitude $> 22.5^\circ$) the warm season is defined from March to October in the Northern Hemisphere and from September to April in the Southern Hemisphere, whereas in the tropics all months are considered. Greenland and desert regions are masked.



50

Figure S6: Intermodel differences in the interannual correlation between detrended NBP and soil moisture. The correlation is computed from the detrended time series of annual average NBP and annual average warm season SM. In the extratropics (latitude > 22.5°) the warm season is defined from March to October in the Northern Hemisphere and from September to April in the Southern Hemisphere, whereas in the tropics all months are considered. Greenland and desert regions are masked.



55

Figure S7: Similar to Fig. S5 but for the covariance between detrended NBP and temperature.

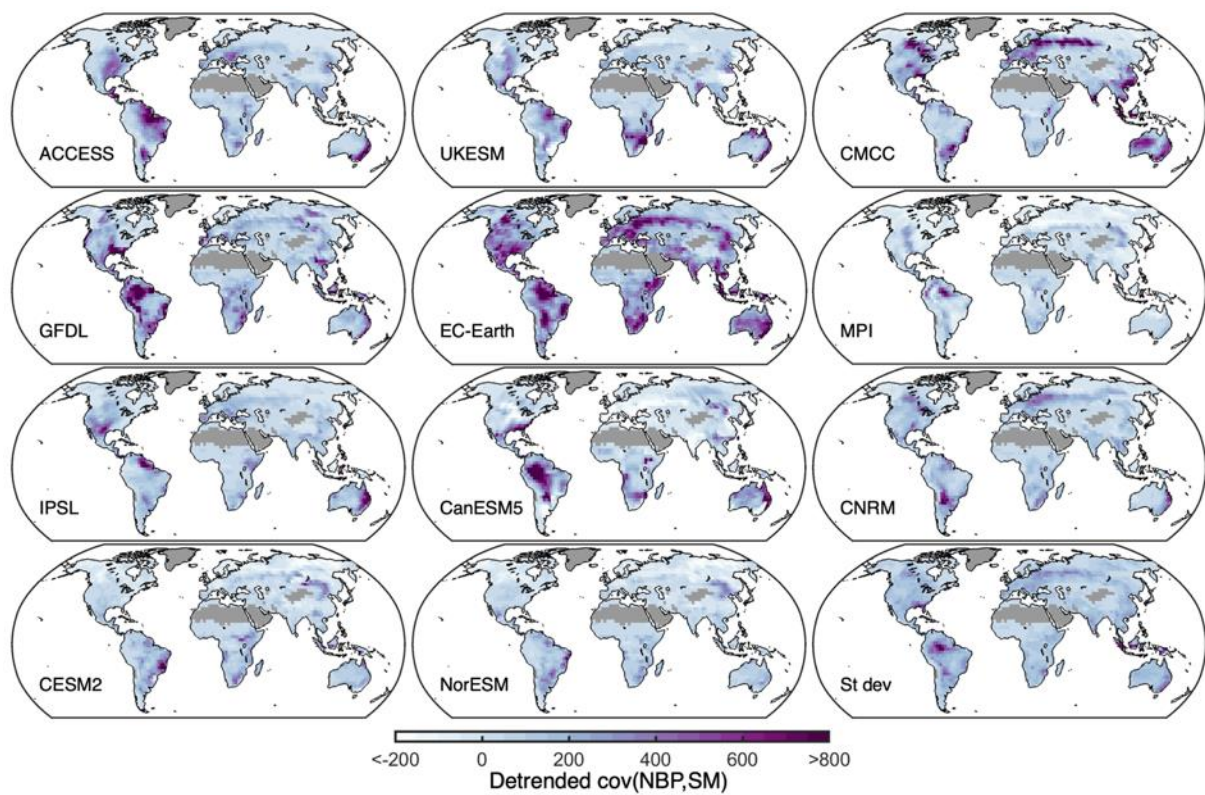
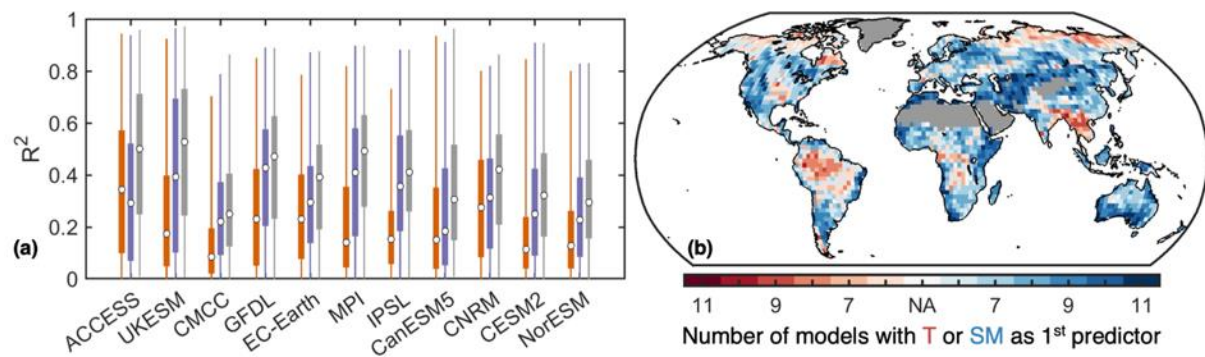


Figure S8: Similar to Fig. S6 but for the covariance between detrended NBP and soil moisture.



60 Figure S9: Similar to Fig. 4 but when considering soil moisture down to 1 m depth instead of the top 30 cm.

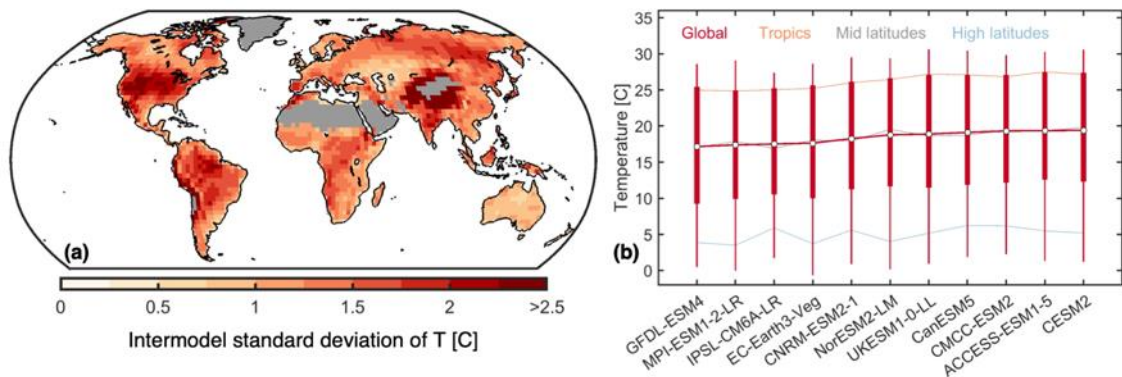


Figure S10: Intermodel differences in average warm-season temperature. (a) Intermodel standard deviation of long-term average T for the period 2015–2100. (b) Distribution of T from all land grid cells. Antarctica, Greenland, and desert regions are omitted. The marker indicates the median T, the boxes span the interquartile range, and the whiskers span from the 5th to the 95th percentile. Additional lines indicate the median T from land grid cells across the tropics, mid latitudes, and high latitudes.

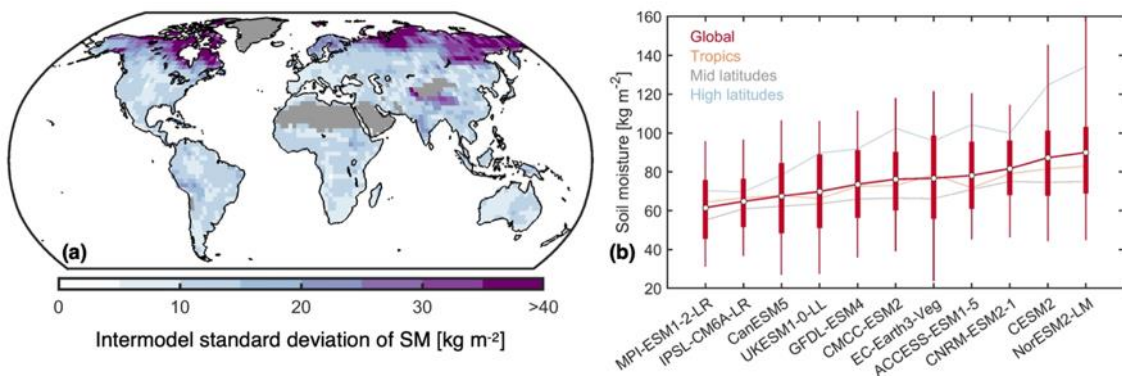


Figure S11: Intermodel differences in average warm-season soil moisture. (a) Intermodel standard deviation of long-term average SM for the period 2015–2100. (b) Distribution of SM from all land grid cells. Antarctica, Greenland, and desert regions are omitted. The marker indicates the median SM, the boxes span the interquartile range, and the whiskers span from the 5th to the 95th percentile. Additional lines indicate the median SM from land grid cells across the tropics, mid latitudes, and high latitudes.

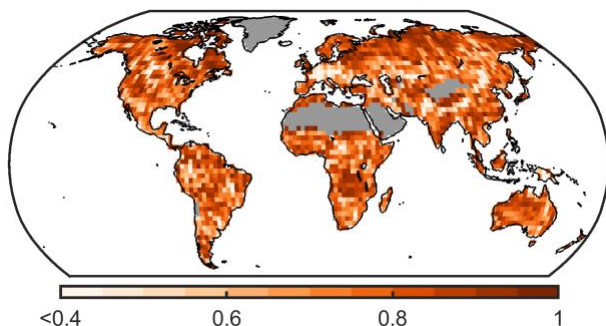
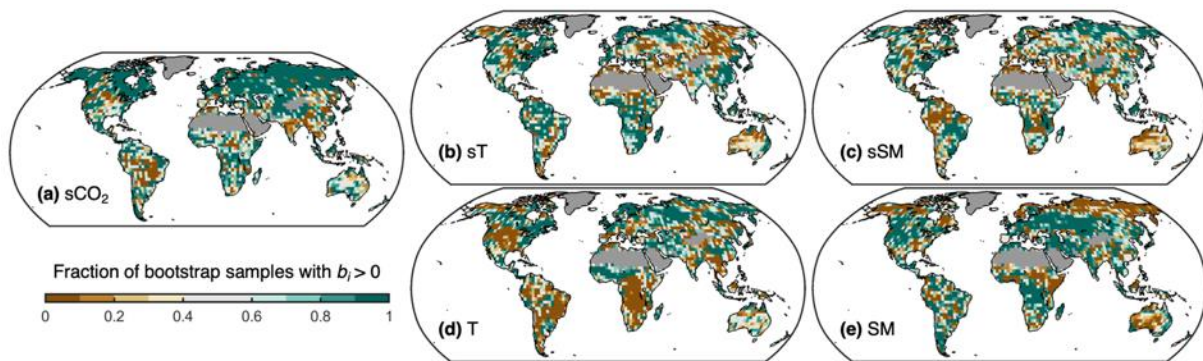


Figure S12: Pearson correlation between projected cumulative NBP from Earth system models and from the multiple linear regression. Cumulative NBP corresponds to the period 2015–2100. Greenland and desert regions are masked.



75 **Figure S13: Robustness of the influence of model characteristics on projected cumulative NBP.** Fraction of 200 bootstrap samples
 with a positive regression coefficient b_i for (a) sensitivity to CO_2 concentration (sCO_2), (b) sensitivity to temperature (sT), (c) sensitivity to
 soil moisture (sSM), (d) long-term warm season average temperature (T), and (e) long-term warm season average soil moisture (SM). In
 this case the multiple linear regression at each grid cell is fitted considering only the covariance or only the correlation (whichever has the
 strongest absolute correlation with projected cumulative NBP) to represent sT and sSM . If both the correlation and the covariance are
 80 considered as in Eq. 1 of the article, then the signs of their corresponding regression coefficients b_i are less informative regarding the net
 effect of sT and sSM on cumulative NBP. Greenland and desert regions are masked.

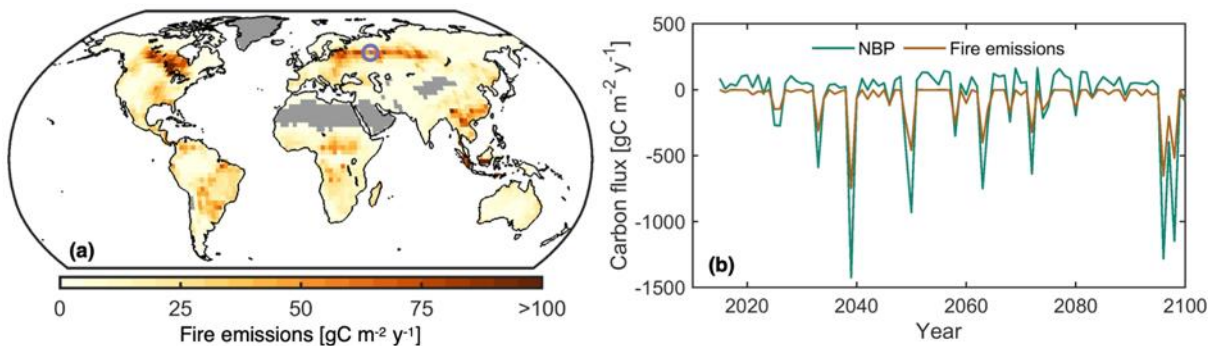


Figure S14: Carbon fire emissions from the CMCC-ESM2 model. (a) Long-term average fire emissions for the period 2015–2100.
 Greenland and desert regions are masked. (b) Temporal evolution of NBP and fire emissions for the high latitude boreal forest grid cell
 85 indicated in the map. A negative value indicates a carbon flux from land to the atmosphere.